

Polyaniline Coated Ethyl Cellulose with Improved Hexavalent Chromium Removal

Bin Qiu,^{†,‡} Cuixia Xu,^{†,§} Dezhi Sun,^{*,‡} Huan Yi,^{||} Jiang Guo,[†] Xi Zhang,[†] Honglin Qu,[†] Miguel Guerrero,[†] Xuefeng Wang,^{*,||} Niyoyankunze Noel,[⊥] Zhiping Luo,[⊥] Zhanhu Guo,^{*,†} and Suying Wei^{*,†,§}

[†]Integrated Composites Laboratory (ICL), Dan F. Smith Department of Chemical Engineering and [§]Department of Chemistry and Biochemistry, Lamar University, Beaumont, Texas 77710 United States

[‡]College of Environmental Science and Engineering, Beijing Forestry University, Beijing, 100083 China

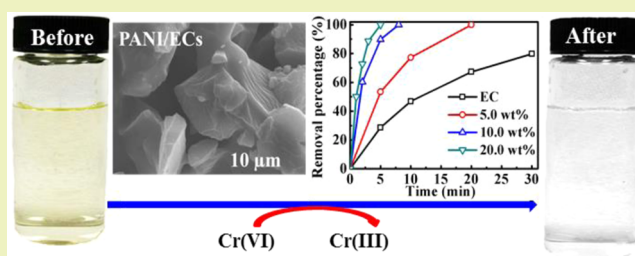
^{||}Department of Chemistry, Tongji University, Shanghai, 200092 China

[⊥]Department of Chemistry and Physics, Fayetteville State University, Fayetteville, North Carolina 28301 United States

S Supporting Information

ABSTRACT: The ethyl celluloses (ECs) modified with 5.0, 10.0, and 20.0 wt % polyaniline (PANI) (PANI/ECs) prepared by homogeneously mixing the EC and PANI formic acid solutions have demonstrated a superior hexavalent chromium (Cr(VI)) removal performance to that of pure EC. Having an increased Cr(VI) removal percentage with increased PANI loading, the PANI/ECs with 20.0% PANI loading were noticed to remove 2.0 mg/L Cr(VI) completely within 5 min, much faster than the pristine EC (>1 h). A chemical redox of Cr(VI) to Cr(III) by the active functional groups of PANI/ECs was revealed from the kinetic study. Meanwhile, isothermal study demonstrated a monolayer adsorption behavior following the Langmuir model with a calculated maximum absorption capacity of 19.49, 26.11, and 38.76 mg/g for the 5.0, 10.0, and 20.0 wt % PANI/ECs, much higher than that of EC (12.2 mg/g). The Cr(VI) removal mechanisms were interpreted considering the functional groups of both PANI and EC, the valence state fates of Cr(VI), and the variation of solution acidity.

KEYWORDS: Cellulose nanocomposites, Polyaniline, Chromium removal, Redox, Adsorption



INTRODUCTION

Chromium is a common contaminant in surface- and groundwater because it is widely used in electroplating, printing, pigments, and other industries.¹ Chromium is classified as one of the most toxic materials in wastewater.^{2,3} The US Environmental Protection Agency (EPA) has issued a maximum concentration of 100 $\mu\text{g/L}$ for total chromium according to the national primary drinking water regulations. The World Health Organization has recommended that the maximum allowable concentration of Cr(VI) in drinking water be 50 $\mu\text{g/L}$. Therefore, its removal from solution is of great significance. In an aqueous environment, chromium usually exists in hexavalent Cr(VI) and trivalent Cr(III) forms. The Cr(VI) has been proven to be more hazardous for living beings and human health, because it can diffuse in the forms of CrO_4^{2-} and HCrO_4^- through the cell membrane, and subsequently oxidize the biological molecules.⁴ Recently, various techniques have been developed for Cr(VI) removal from wastewater or groundwater, including ion exchange,⁵ membrane separation,⁶ electro-reduction,⁷ and adsorption.⁸ Among these techniques, the adsorption is considered to be the most popular method due to its low cost and high removal efficiency.

The Cr(VI) is acutely toxic and carcinogenic, and it is also highly soluble and mobile in an aqueous environment.

Contrarily, the Cr(III) is relatively nontoxic and immobile. It does not readily migrate in groundwater since it usually precipitates as hydroxides and oxides.⁷ Therefore, reducing Cr(VI) to Cr(III) and then absorbing Cr(III) on a solid adsorbent surface is a more effective approach for remediating Cr(VI) contamination. As documented, the most important forms of Cr(VI) in a solution are chromate (CrO_4^{2-}), dichromate ($\text{Cr}_2\text{O}_7^{2-}$), and hydrogen chromate (HCrO_4^-).⁹ These ion forms are related to the pH value of solution and to the total chromium concentration in the solution. HCrO_4^- and H_2CrO_4 are the dominant forms when the pH is lower than 6.8, while only CrO_4^{2-} is stable when the pH is above 6.8. Cr(VI) removal performance works best when it is obtained in acidic solutions.^{9–11} As reported, HCrO_4^- exhibits a higher redox potential (1.33 eV) in acidic solutions, leading to an easy reduction to Cr(III).⁹ Lots of materials have been used as the electron donors for this reduction reaction, such as zero-valent iron (ZVI),¹² Fe_3O_4 ,^{10,12–14} zero-valent Al (ZVAL),⁴ polymers,^{9,13} and biomass, e.g. cellulose.^{15,16} ZVI and Fe_3O_4 have good magnetic properties that are widely used for Cr(VI)

Received: May 14, 2014

Revised: June 5, 2014

Published: June 9, 2014

removal due to their easy separation.^{10,12–14} However, there are two challenges for using ZVI and Fe_3O_4 as the active components to remove Cr(VI). One is the easy dissolution of the ZVI/ Fe_3O_4 in acidic solution.¹² Therefore, the ZVI/ Fe_3O_4 have often been supported on the surface of mesoporous materials such as active carbon,¹⁷ carbon nanotubes,¹⁸ and resin.¹⁹ Moreover, long chain polymers were coated on the surface of ZVI and Fe_3O_4 to prevent iron from dissolving and to improve the Cr(VI) removal efficiency, especially for polymers containing amine groups, such as chitosan,²⁰ and polyaniline.¹³ The second challenge is the Cr(III)–Fe(III) precipitation on the adsorbent surface, which prevents the electron transfer from the internal particles to the Cr(VI) in solution and thus leads to a decreased Cr(VI) reduction. Moreover, the amine and hydroxyl groups on the chitosan and polyaniline were found to inhibit the formation of Cr(III) precipitation due to their high efficiency in chelating the Fe(III) ions,²¹ resulting in the Cr(III) release into solution. Other processes are thus needed for further treatment of the released Cr(III).

Besides these materials, cellulose was also used as an adsorbent to remove organic and heavy metals pollutants from wastewater. Cellulose is abundant in nature and contains lots of active sites, i.e. hydroxyl groups, which can provide active adsorption sites for heavy metal adsorption.^{15,16} Cellulose can also act as an electron donor for the Cr(VI) reduction. Cr(VI) can be reduced to Cr(III) by the hydroxyl groups on the surface of cellulose. However, the lower adsorption capacity and removal rate limit its application. In order to improve its removal rate and removal capacity, cellulose was modified with polymers containing amine groups.²² A surface initiated polymerization method was often used to modify cellulose. In the synthesized composites, the cellulose, hidden by the polymers, serves as a support for the polymers rather than participates in the reaction with Cr(VI).^{22,23} To improve the removal capacity, it is of importance to make the groups of cellulose also act as available active sites for Cr(VI) reduction and adsorption.

Polymers containing the abundant amine groups can act as the electron donors for Cr(VI) reduction.^{17,13,23} Among the polymers, polyaniline (PANI), as a conductive polymer, has been widely used for various fields. It has three redox states based on the ratio of the amine group and imine group,²⁴ e.g. fully reduced leucoemeraldine base (LB), half oxidized emeraldine base (EB), and fully oxidized pernigraniline base (PB). Therefore, heavy metals with higher valence states can be reduced to low valence states by the oxidation of the LB and EB forms to PB form.^{13,25} Moreover, PANI has a good resistance against acid or alkaline.¹¹ This makes PANI more suitable for Cr(VI) removal since the Cr(VI) can be efficiently removed in acidic solutions, especially with pH ranging from 1 to 3.^{9–11} However, there is a recycling and regeneration challenge for PANI application due to the small size of PANI.²⁶ Coating PANI on cellulose is one of the strategies to improve the recycle and reuse capability. The PANI/cellulose composites have been synthesized by a surface initiated polymerization method and were used to reduce Cr(VI).^{22,27} The active groups, i.e. –OH, of the cellulose were wrapped by the in situ formed polyaniline, which inhibits their performance on the Cr(VI) removal. The Cr(VI) removal mechanisms involving the polyaniline and cellulose were not reported.

In this study, the composites of PANI and ethyl cellulose (EC) (PANI/EC) were synthesized by homogeneously mixing

the PANI and EC formic acid solutions. The PANI loading was controlled at 5.0, 10.0, and 20.0 wt %. The morphology was characterized by a scanning electron microscope (SEM). The functional group was determined by Fourier transform infrared spectroscopy (FT-IR) and X-ray photoelectron spectroscopy (XPS). The hydrophilic property of EC and PANI/ECs was determined by contact angle measurements with deionized water. The thermal stability was evaluated by thermogravimetric analysis (TGA). The Cr(VI) removal performances were explored by adsorption batch assays. The effects of the PANI loading, treatment time, initial pH value, and Cr(VI) concentration on the Cr(VI) removal were investigated. Kinetics and isothermal adsorption behaviors of the adsorbents were studied as well. Meanwhile, the mechanisms involved in the Cr(VI) removal by PANI/EC were investigated based on the results from FT-IR and XPS.

EXPERIMENTAL SECTION

Materials. Ethyl cellulose (EC, with 48–49.5% ethoxy content), aniline ($\text{C}_6\text{H}_7\text{N}$, 99.9%), ammonium persulfate (APS, $(\text{NH}_4)_2\text{S}_2\text{O}_8$, 98%), and *p*-toluene sulfonic acid (PTSA, $\text{C}_7\text{H}_8\text{O}_3\text{S}$, >98.5%) were purchased from Sigma-Aldrich. Potassium dichromate ($\text{K}_2\text{Cr}_2\text{O}_7$, 99%) and 1,5-diphenylcarbazide (DPC, 98%) were purchased from Alfa Aesar Company. Formic acid (CH_2O_2 , >95%) and phosphoric acid (H_3PO_4 , 85 wt %) were obtained from Fisher Scientific. All the chemicals were used as-received without any further treatment.

Preparations of PANI and PANI/ECs. PANI was synthesized by the method described in the previous work.¹³ Briefly, PTSA (30.0 mmol) and APS (18.0 mmol) were added into 200 mL deionized water in an ice–water bath for 1 h sonication. Then the aniline aqueous solution (36.0 mmol in 50.0 mL deionized water) was mixed with the above solution and was sonicated continuously for an additional hour in an ice–water bath for polymerization. The solid product was vacuum filtered and washed with deionized water until pH was ~ 7.0 and was further washed with methanol to remove any possible oligomers. The final PANI product was dried at 50 °C overnight. The PANI was then dissolved in formic acid to obtain a concentration of 1.0 wt % PANI solution. The formic acid unravels the randomly entangled PANI chains and dissolves the polymer down to the chain level.²⁸ A 4.0 g portion of EC was dissolved in 20.0 mL formic acid, and the EC solution was mixed with 5.4, 11.2, 17.6, and 25.0 g PANI solution, respectively, to obtain the PANI/ECs with 5.0, 10.0, 15.0, and 20.0 wt % PANI loadings. The mixed solutions were stirred and heated at 50 °C until formic acid was totally volatilized. The PANI/ECs were dried at room temperature for further usage.

Cr(VI) Removal. The effect of PANI loading on the Cr(VI) removal was investigated by using 60.0 mg PANI/ECs to treat 2.0 mg/L Cr(VI) solutions (20.0 mL, pH = 1.0) for 5 min. Then the solutions were taken out and determined for Cr(VI) concentrations. For comparison, the as-received EC (60.0 mg) was used to treat 20.0 mL Cr(VI) solution at pH 1.0 with an initial Cr(VI) concentration of 2.0 mg/L for 5 min.

The effect of initial pH on the Cr(VI) removal was investigated using the PANI/ECs with a 20.0 wt % PANI loading. The pH values of 1.0, 2.0, 3.0, 5.0, 7.0, 9.0, and 11.0 were selected. The initial pH of Cr(VI) solutions was adjusted by NaOH (1.0 mol/L) and H_2SO_4 (1.0 mol/L) with a pH meter (Vernier Lab Quest with pH-BTA sensor). The PANI/ECs (60.0 mg) were added in 20.0 mL Cr(VI) solutions (2.0 mg/L) for 5 min.

The effect of initial Cr(VI) concentration on the Cr(VI) removal was investigated by using PANI/ECs (60.0 mg) to treat Cr(VI) solutions (20.0 mL, pH = 1.0) with Cr(VI) concentration varying from 1.0 to 200.0 mg L^{-1} for 30 min.

For kinetic study purpose, the synthesized PANI/ECs were used to treat 20.0 mL Cr(VI) solution with an initial Cr(VI) concentration of 20.0 mg/L at a pH of 1.0, 2.0, and 3.0. The Cr(VI) concentration and the pH values were determined at different time intervals.

To determine the total Cr concentration in solution after Cr(VI) removal, the solution was first oxidized by the oxidant APS in an acidic condition at 100 °C.²² APS will oxidize Cr(III) to Cr(VI), and therefore, the Cr(VI) concentration was the total Cr concentration. The Cr(III) concentration was calculated from the difference between the total Cr and Cr(VI) concentration. All the Cr(VI) removal tests were conducted at room temperature.

The concentration of Cr(VI) in solution was determined by the colorimetric method² using the obtained standard fitting equation: $A = 9.7232 \times 10^{-4}C$, where C is the concentration of Cr(VI) and A is the absorbance at 540 nm obtained from the UV-vis test.

The Cr(VI) removal percentage ($R\%$) is calculated using eq 1:

$$R\% = \frac{C_0 - C_e}{C_0} \times 100\% \quad (1)$$

where C_0 and C_e (mg/L) are the Cr(VI) concentrations in the solution before and after the treatment, respectively. The removal amount (Q , mg/g) is quantified by eq 2:

$$Q = \frac{(C_0 - C_e)V}{m} \quad (2)$$

where, V (L) represents the volume of Cr(VI) solution and m (g) is the mass of the used PANI/ECs.

Characterizations. The morphology of the PANI/ECs was characterized by a JEOL field emission scanning electron microscope (SEM, JSM-6700F system). The functional groups were characterized by the Fourier transform infrared spectroscopy (FT-IR, a Bruker Inc. Vector 22 coupled with an ATR accessory) in the range of 600–4000 cm^{-1} at a resolution of 4 cm^{-1} . The thermal stability of the as-received EC, PANI/ECs before and after treated with Cr(VI) was conducted in a thermogravimetric analysis (TGA, TA Instruments, Q-500) under the air condition with a heating rate of 10 °C/min and an air flow rate of 60 mL/min from 25 to 800 °C. The X-ray photoelectron spectroscopy (XPS) measurements were performed in the Kratos AXIS 165 XPS/AES instrument using a monochromatic Al K radiation to determine the elemental compositions and the valence state of chromium. The N 1s, C 1s, O 1s, and Cr 2p peaks were deconvoluted into the components consisting of a Gaussian line shape Lorentzian function (Gaussian = 80%, Lorentzian = 20%) on a Shirley background. The hydrophilic property of the PANI/ECs was determined by using a contact angle analyzer (contact angle analyzer, Future Digital Scientific Corp.) with deionized water.

RESULTS AND DISCUSSION

Characteristics of PANI/ECs. The morphologies of EC and the synthesized PANI/ECs were observed by SEM. The EC particle has a much rougher surface (Figure 1A and B). The PANI nanoparticles have an average diameter of 500 nm (Figure S1). The white EC particles became black ones after modified with PANI. The PANI/ECs (Figure 1C and D) exhibit a particle structure with an average diameter of 10 μm and are much smoother than the as-received EC, indicating that the PANI has been well mixed and been successfully grafted on EC.

The functional groups of pure PANI, EC, and synthesized PANI/ECs with different PANI loadings were characterized by FT-IR. Figure 2a shows the spectra of pure PANI. Strong absorption peaks at 1562, 1459, and 1291 cm^{-1} are assigned to the stretching vibration of C–N in N=Q=N, N–B–N, and B–NH–B (Q, quinoid ring; B, benzenoid ring),^{29,30} respectively. The peak at 752 cm^{-1} is due to the out-of-plane bending of C–H in the substituted benzenoid ring.²⁹ The ratio of N–B–N (1459 cm^{-1}) to N=Q=N (1562 cm^{-1}) can serve as an indication of half oxidized emeraldine base (EB) form of PANI. The peaks ranging from 3200 to 3500 cm^{-1} may be due to the overlapping of –OH and –NH stretching,^{15,16} and the

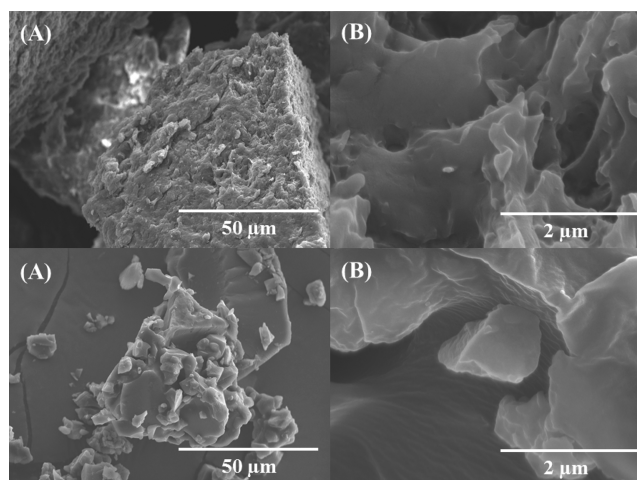


Figure 1. SEM images of (A and B) ethyl cellulose and (C and D) PANI/ECs with a 20.0 wt % PANI loading.

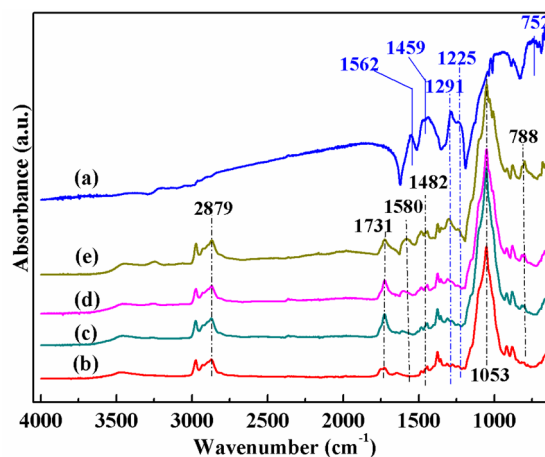


Figure 2. FT-IR spectra of (a) PANI, (b) EC, and PANI/ECs with a PANI loading of (c) 5.0, (d) 10.0, and (e) 20.0 wt %.

3250 cm^{-1} is characteristic of –NH stretching vibration.⁹ Figure 2b shows the characteristic peaks of EC. The peaks located at 3480 and 2879 cm^{-1} are corresponding to the –OH stretching vibration and C–H vibration of CH_2 groups in EC.²³ The peak at 1053 cm^{-1} represents the C–OH deformation vibrations and/or C–O stretching vibrations in EC.¹⁶ As shown in Figure 2c–e, all the characteristic peaks corresponding to the groups of PANI appear in the FT-IR spectra of PANI/ECs. The characteristic peaks at 1562 and 1459 cm^{-1} corresponding to the C–N in N=Q=N and N–B–N shifted to bigger wavenumbers (1580 and 1482 cm^{-1}), while the peak (1291 cm^{-1}) corresponding to the stretching vibration of C–N in B–NH–B had no change. Also, the peaks at 1562 and 1459 cm^{-1} shifted to bigger wavenumbers, indicating strong intermolecular hydrogen bonds between PANI and EC after modification.

Figure 3 shows the C 1s and the N 1s XPS spectra of the synthesized PANI/ECs with 20.0 wt % PANI loading. The C 1s peak (Figure 3A) was deconvoluted to three major components with the binding energy peaks at 281.8, 283.4, and 284.8 eV, which are attributed to the C–C, C–N, and C–O,³¹ respectively. The C–N peak suggested the presence of PANI in the composites. The nitrogen-containing groups were determined by the N 1s XPS spectra (Figure 3B). It was deconvoluted into three major components with the peaks at

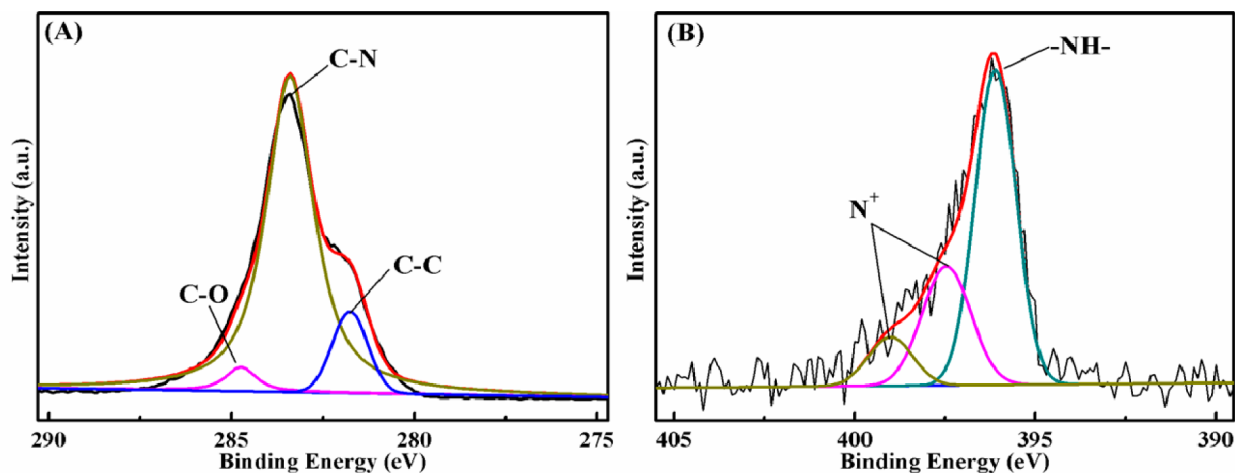


Figure 3. (A) C 1s and (B) N 1s XPS spectra of synthesized PANI/ECs with 20.0 wt % PANI loading.

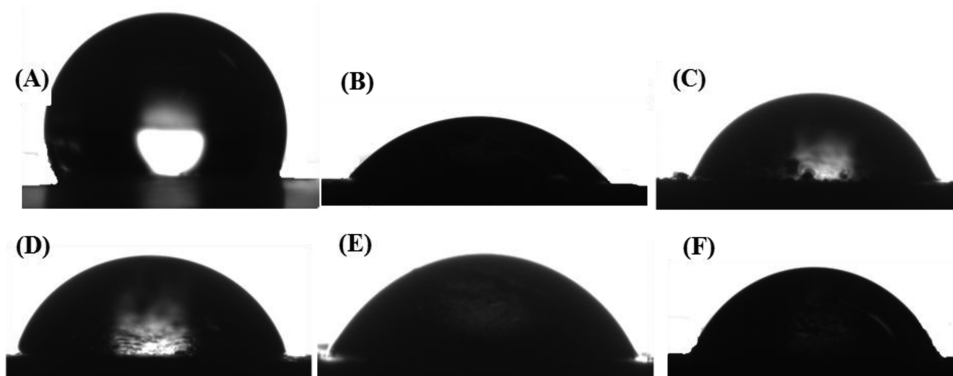


Figure 4. Images of the contact angle of (A) EC, (B) PANI, PANI/ECs with a PANI loading of (C) 5.0, (D) 10.0, and (E) 20.0 wt %, and (F) PANI/ECs (20.0 wt %) treated with Cr(VI).

396.1, 397.5, and 399.0 eV, which are related to undoped amine ($-\text{NH}-$), doped imine ($-\text{N}=\text{}$), and doped amine group, respectively. All the peaks shifted to lower binding energies.³² The greater proportion of amine groups in the N 1s component confirms that the EB form of PANI in the PANI/ECs composite,³³ which is consistent with the result based on FT-IR spectra of synthesized PANI/ECs (Figure 2c–e).

Figure 4 shows the images of the contact angles for EC and PANI/ECs with different PANI loadings. Pure EC (Figure 4A) has a contact angle of 113.1° with deionized water, indicating a hydrophobic nature of EC. The result is different from the cellulose nanofibers, which are superhydrophilic and tend to absorb moisture due to high density of hydroxyl groups.³⁴ For EC used in this study, 48% hydroxyl groups were replaced by ethyl groups, leading to the increase in hydrophobicity. The PANI, which contains abundant amine groups, has a contact angle of 51.5° (Figure 4B), demonstrating the hydrophilic property of PANI. The contact angles of PANI/ECs (Figure 4C–E) is decreased with increasing the PANI loading (71.5° , 67.6° , and 60.1° for PANI/ECs with a PANI loading of 5.0, 10.0, and 20.0 wt %, respectively). This indicates that PANI has improved the hydrophilic property of the composites, which may enhance the contact of adsorbent with pollutants and can accelerate the pollutant removal from solution.

The thermal stability of the synthesized PANI/ECs was investigated by TGA. As shown in Figure 5a, two-stage weight losses were observed for the as-received EC. There was moisture lost before 120°C , and then, the oxidative

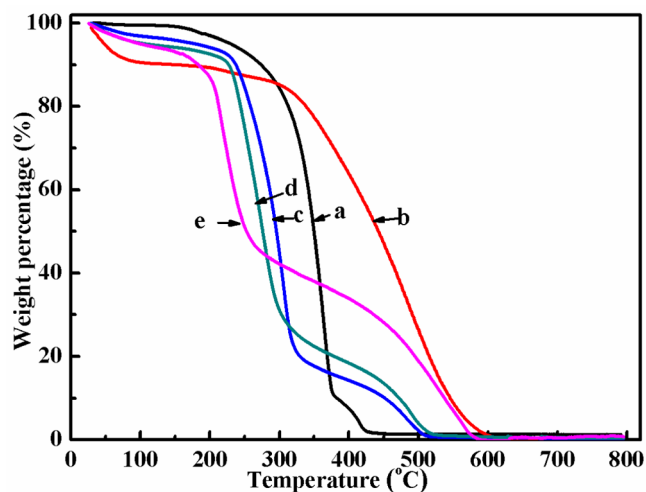


Figure 5. TGA curves of (a) EC, (b) PANI, and PANI/ECs with a PANI loading of (c) 5.0, (d) 10.0, and (e) 20.0 wt %.

decomposition of EC chains was achieved from 200 to 400°C .³⁵ Figure 5b shows three-stage weight losses for pure PANI, consistent with the previous reports.¹³ The weight loss before 120°C is attributed to the moisture loss. The others are at 250 and 450°C due to the elimination of dopant anion and the thermal degradation of PANI chains,¹³ respectively. The thermal stability of PANI/ECs (Figure 5c–e) decreases with

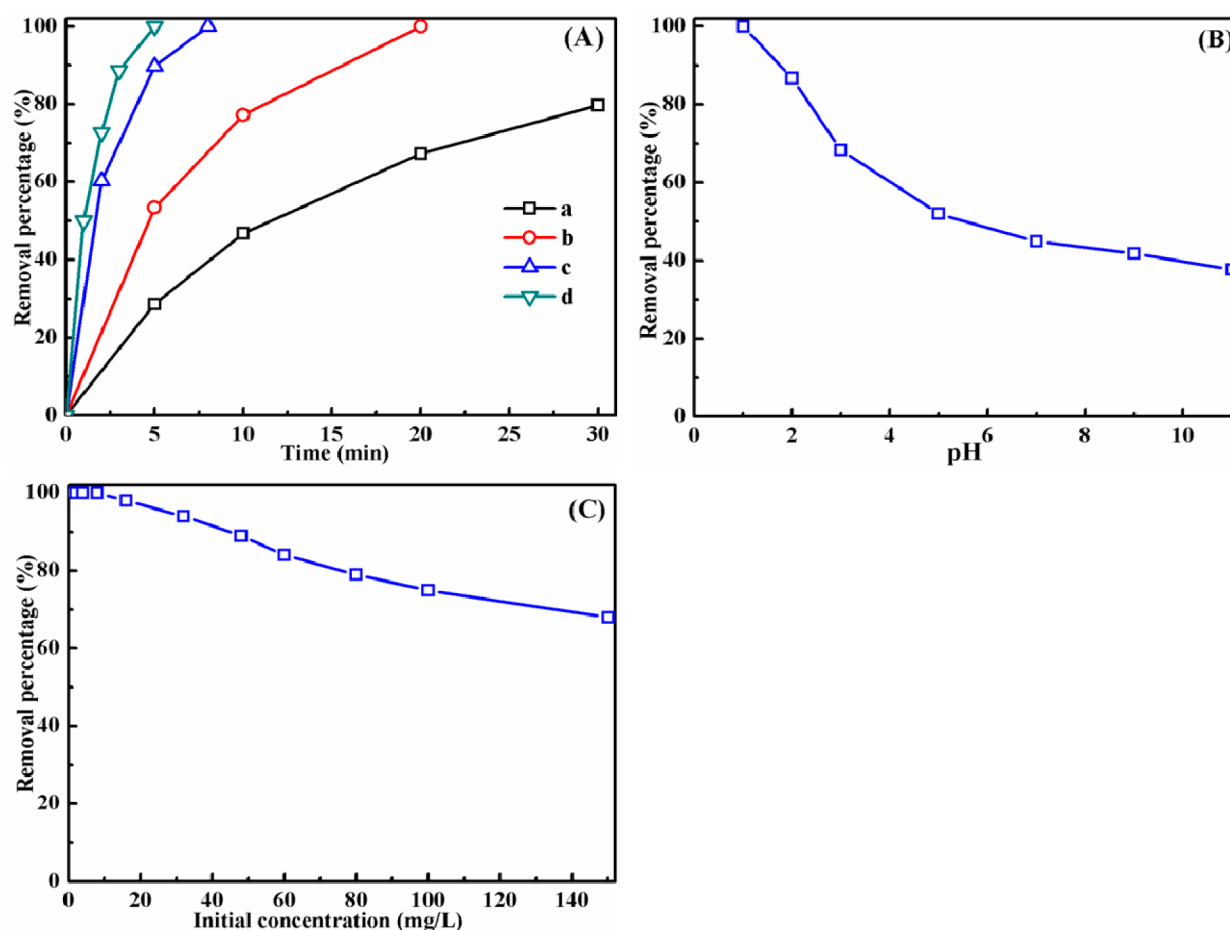


Figure 6. (A) Cr(VI) removal by (a) cellulose and PANI/ECs with a PANI loading of (b) 5.0, (c) 10.0, and (d) 20.0 wt %. [Cr(VI)] = 2.0 mg/L, pH = 1.0, adsorbent dosage = 60 mg, volume = 20 mL. (B) pH effect on Cr(VI) removal by PANI/ECs with 20.0 wt % PANI loading. [Cr(VI)] = 2.0 mg/L, time = 5 min, adsorbent dosage = 60 mg, volume = 20 mL. (C) Cr(VI) concentration effect on Cr(VI) removal by PANI/ECs with 20.0 wt % PANI loading. pH = 1.0, time = 30 min, adsorbent dosage = 60 mg, volume = 20 mL.

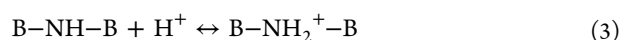
increasing the PANI loading. It is noticed that the weight loss of PANI/ECs before 120 °C is more than that of pure EC and increases with increasing the PANI loading.

Cr(VI) Removal by PANI/ECs. *Cr(VI) Removal Investigations.* The effect of PANI loading on the Cr(VI) removal from wastewater was investigated (Figure 6A). The removal rate of Cr(VI) by the PANI/ECs increases with increasing the PANI loading, indicating that the PANI plays an important role in the Cr(VI) removal. The LB form of PANI (Figure 2 and 3) has lots of amine groups that have a higher reductive capability and can effectively reduce the Cr(VI) to Cr(III). A 2.0 mg/L portion of Cr(VI) can be completely removed by PANI/ECs with a 20.0 wt % PANI loading within 5 min (Figure 6A d). For comparison, only 40% of Cr(VI) can be removed from solution in 5 min and ~75% of Cr(VI) is removed within 30 min by EC (Figure 6A a). The Cr(VI) removal rate by PANI/ECs is observed much faster than that of pure EC (>1 h), cellulose modified with silica (30 min),³⁶ 38 wt % methyltriethylammonium chloride (30 min),³⁷ 70 wt % tetrabutylammonium iodide (30 min)³⁸ and other adsorbents such as N-doped porous carbon (60 min),³⁹ zerovalent magnesium (60 min),⁴⁰ and chitosan beads-supported Fe⁰ (several hours).⁴¹ The performance is as good as magnetic graphene nanocomposites (5 min)² and magnetic polyaniline nanocomposites (5 min).¹³ However, the PANI loading was up to 70% in the magnetic nanocomposites, which is much higher than 20.0 wt % PANI loading

synthesized in this study. This indicates that the PANI/ECs can be used as the adsorbent for a faster Cr(VI) removal from polluted wastewater. Moreover, a little longer time was needed for PANI/ECs with lower PANI loadings. Periods of 8 and 20 min were needed for the complete Cr(VI) removal by PANI/ECs with a PANI loading of 10.0 and 5.0 wt % (Figure 6A b and c). PANI/ECs with a higher PANI loading contain more amine groups (Figure 2). On one hand, the amine groups act as active sites for Cr(VI) adsorption by the electron attraction between the protonated amine groups and negatively charged CrO₄²⁻ under acidic condition. On the other hand, the hydrophilic property of the synthesized PANI/ECs was improved with increasing the PANI loading (Figure 4). The improved hydrophilic property enhanced the Cr(VI) transfer from solution to the surface of adsorbent, which is consistent with the fact that a shorter time was needed for a complete Cr(VI) removal by PANI/ECs with a higher PANI loading. Therefore, the PANI/ECs composites with a PANI loading of 20.0 wt % were selected for further study of Cr(VI) removal.

The effect of initial pH value on the Cr(VI) removal was investigated by using PANI/ECs with a 20.0 wt % PANI loading as the adsorbent. Figure 6B shows a highly pH dependent Cr(VI) removal. The Cr(VI) removal percentage decreases with increasing pH value. 100% of Cr(VI) removal is achieved at pH 1.0, while only ~40% of Cr(VI) can be removed by PANI/ECs at pH 11.0. A similar trend was also observed

during the Cr(VI) removal by cellulose coated with tetrabutylammonium iodide³⁸ and other adsorbents, e.g. magnetic PANI nanocomposites.¹³ Two possible reasons are proposed to account for the high Cr(VI) removal percentage by PANI/ECs in acidic solutions. Abundant amine groups (Figure 2) that are distributed on the surface of PANI/ECs composites can be easily protonated and be positively charged. A lower pH is ideal for protonation of amine groups, while higher pH is for deprotonation. The reactions in eqs 3 and 4 indicate the protonation and deprotonation of the amine groups of PANI/ECs in acidic and basic solutions (B is the benzenoid ring).



The PANI/ECs surface was then positively charged under the acidic conditions⁴² through the protonation of amine groups. After protonation, the surface of PANI/ECs was positively charged. Higher PANI loading leads to higher positive charges on the adsorbent surface, which improves the electrostatic attraction with the negatively charged Cr(VI) species (CrO_4^{2-} and HCrO_4^-). At higher pH values, OH^- may be adsorbed on the surface of PANI/ECs through the hydrogen bond, leading to the negatively charged sites. It would be repulsion between these negatively charged sites and the negatively Cr(VI) species, which consequently decrease the Cr(VI) adsorption rate and amount. The other reason is that the HCrO_4^- can be more easily reduced to Cr(III) under acidic condition. The most important forms of Cr(VI) in the solution are chromate (CrO_4^{2-}), dichromate ($\text{Cr}_2\text{O}_7^{2-}$), and hydrogen chromate (HCrO_4^-), which are related to the pH value and total Cr concentration of the solution. The HCrO_4^- and H_2CrO_4 are the dominant forms when pH is lower than 6.8, while only stable CrO_4^{2-} when pH is above 6.8. As reported, the HCrO_4^- with a higher redox potential (1.33 eV) in an acidic solution can be easily reduced to Cr(III) by the oxidation of active groups of adsorbent.

Figure 6C shows the effect of initial Cr(VI) concentration on the Cr(VI) removal by PANI/ECs with 20.0 wt % PANI loading. It is obvious that 8.0 mg/L Cr(VI) can be completely removed from a solution with an initial pH of 1.0 by adding 60 mg PANI/ECs within 5 min. The removal percentage then decreases with increasing the initial Cr(VI) concentration. The decrease in Cr(VI) removal percentage is mainly due to the limitation of active adsorption sites on the surface of PANI/ECs. Moreover, the high redox potential of solution with high Cr(VI) concentration leads to over oxidation and degradation of PANI. However, ~70% Cr(VI) can be removed by PANI/ECs with a 20.0 wt % PANI loading even when the initial Cr(VI) concentration was up to 160 mg/L.

Adsorption Kinetics and Isotherms. Kinetics models are used to find the potential rate-controlling step involved in the Cr(VI) removal process by PANI/ECs. It is observed from Figure 6A that the adsorption rate of Cr(VI) by PANI/ECs is rapid during the initial reaction stage, and then becomes gradually slow. Similar kinetics was also observed for the Cr(VI) adsorption for many adsorbents, e.g. chitosan,²⁰ PANI,¹³ and polyethylenimine functionalized biomass.⁹ In this study, two models, pseudo-first-order and pseudo-second-order, were used to evaluate the kinetics of Cr(VI) removal by PANI/ECs with different PANI loadings. The PANI/ECs were used to adsorb Cr(VI) from artificial wastewater with an initial Cr(VI) concentration of 20.0 mg/L. The adsorption reached

equilibrium within 45 min. More importantly, ~50% of Cr(VI) could be removed within 10 min. As shown in Table 1, the

Table 1. Cr(VI) Adsorption Kinetics by PANI/ECs using Pseudo-first-order and Pseudo-second-order Models^a

loading (wt %)	pseudo-first-order		pseudo-second-order		
	equation	$\log\left(\frac{Q_e - Q_t}{Q_e - (k_1/2.303)t}\right) = \log\left(\frac{t/Q_t}{(t/Q_e)}\right) + \frac{1}{k_{ad}Q_e^2}$	R^2	k_{ad} (g/mg-min)	R^2
5.0	k_1 (min ⁻¹)	0.2596	0.7540	0.0207	0.998
10.0		0.3387	0.8530	0.0183	0.997
20.0		0.3921	0.7340	0.0139	0.996

^a Q_t is the Cr(VI) uptake amount on the adsorbent at time t , Q_e is the adsorption capacity at equilibrium, k_1 is the rate constant of pseudo-first-order adsorption. In the pseudo-second-order model, k_{ad} is the rate constant of adsorption.

adsorption processes were found to fit better with pseudo-second-order with a correlation of more than 0.99. The fitness with a pseudo-second-order kinetics indicates that the adsorption rate is controlled by chemical adsorption. This is consistent with the results that the Cr(VI) removal by other adsorbents^{13,20} fits better with pseudo-second-order kinetic, due to the fact that the Cr(VI) reduction reaction was the control step in Cr(VI) removal process. The result is also consistent with the results based on FT-IR (Figure 8) and XPS (Figure 9), showing that the Cr(VI) was reduced to Cr(III) by the oxidation of PANI/ECs.

Various isotherm models including the Langmuir and Freundlich model were used to fit the Cr(VI) removal behavior by PANI/ECs. The Langmuir isotherm is described as eq 5:

$$\frac{C_e}{q_e} = \frac{1}{bq_{max}} + \frac{C_e}{q_{max}} \quad (5)$$

where C_e is the equilibrium concentration (mg/L) of Cr(VI), q_e is the Cr(VI) amount adsorbed at equilibrium (mg/g), q_{max} is the adsorption capacity of PANI/CF(mg/g), and b is a constant (L/mg).

The Freundlich isotherm is an empirical model that considers heterogeneous adsorptive energies on the surface of adsorbent, and it can be described as eq 6:

$$\log q_e = \log k_f + \frac{1}{n} \log C_e \quad (6)$$

where q_e is the amount of Cr(VI) adsorbed on the surface of PANI/CF at equilibrium, C_e is the equilibrium concentration, and k_f and n are constants of the Freundlich model.

The PANI/ECs were used to treat the Cr(VI) solution with Cr(VI) concentrations ranging from 2.0 to 200.0 mg/L at pH 1.0. The fitted results are shown in Figure 7. According to the correlation coefficient values, it can be seen that the Langmuir model fits better for the Cr(VI) adsorption isotherm, indicating that the Cr(VI) adsorption by PANI/ECs is limited with monolayer coverage. The maximum adsorption capacities of Cr(VI) on PANI/ECs with a PANI loading of 5.0, 10.0, and 20.0 wt % calculated from Langmuir model are 19.49, 26.11, and 38.76 mg/g, which is much higher than that of pure EC (12.2 mg/g). The adsorption capacity is higher than the cellulose functionalized by silica (19.46 mg/g),³⁶ tetrabutylammonium iodide (16.67 mg/g)³⁸ and other adsorbents such as the N-doped carbon with magnetic particles (16 mg/g).³⁹ PANI/ECs perform as well as the cellulose grafted with 38 wt

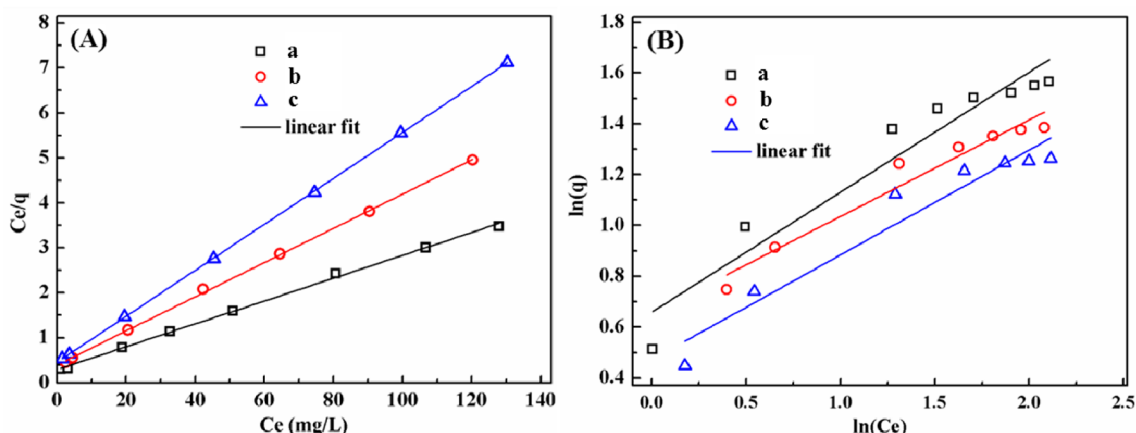


Figure 7. (A) Langmuir and (B) Freundlich isotherms for Cr(VI) removal by PANI/ECs with a PANI loading of (a) 5.0, (b) 10.0, and (c) 20 wt %.

% methyltriethylammonium chloride with an adsorption capacity of 38.94 mg/g.³⁷

Cr(VI) Removal Mechanism by PANI/ECs. The PANI/ECs have demonstrated an effective capability to remove Cr(VI) from polluted solution. The pH value of solution has exerted great influence on the Cr(VI) removal performance. In this study, the mechanisms involved in the Cr(VI) removal were studied by FT-IR and XPS.

Figure 8 shows the FT-IR spectra of PANI/ECs with a 20.0 wt % PANI loading before and after treated with Cr(VI)

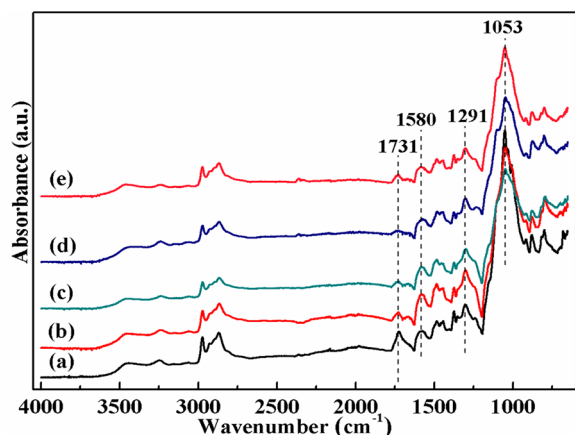


Figure 8. FT-IR spectra of the (a) PANI/ECs with 20.0 wt % PANI loading and PANI/ECs treated with (b) 1.0, (c) 4.0, (d) 32.0, and (e) 80.0 mg/L Cr(VI) solutions at pH 1.0.

solutions at different concentrations. The decrease in absorption at 3250 cm^{-1} after treated with Cr(VI) indicates that the $-\text{NH}$ groups have participated in the adsorption process. The intensities of the two peaks at 1580 and 1482 cm^{-1} decrease with increasing Cr(VI) concentration due to the over oxidation of PANI. The ratio of intensity at 1580 cm^{-1} (imine group) to 1482 cm^{-1} (amine group) increases with increasing Cr(VI) concentration, indicating that the amine group has been oxidized to an imine group and the PANI has been oxidized from EB to PB form (the highest oxidation state of PANI) by Cr(VI). Moreover, the intensity of peak at 1053 cm^{-1} decreases obviously with increasing the Cr(VI) concentration, indicating that the $-\text{OH}$ groups have participated in the Cr(VI) reduction. This is consistent with previous reports that the hydroxyl group is the active site for Cr(VI)

reduction by oxidation to a carboxyl group.^{15,16} This result is consistent with a slightly increased contact angle (68.5°) of PANI/ECs after treatment with Cr(VI) (Figure 4F). The results suggested that both the PANI and EC in the composites have participated in the reduction of Cr(VI), which accounts for the significantly increased removal capacity for PANI/ECs than the as-received EC.

The XPS spectra of Cr 2p, N 1s, and C 1s were used to determine the valence state of chromium, and the functional groups of nitrogen, and carbon on the surface of the PANI/ECs after being treated with 1000 mg/L Cr(VI) solution (Figure 9). Figure 9A shows the XPS Cr 2p spectra of PANI/ECs with 20.0 wt % PANI after treated with 1000 mg/L Cr(VI) solution for 30 min with an initial pH of 3.0. The binding energy peaks of Cr 2p are observed to be located at 576.0 and 585.2 eV, indicating that the chromium can be adsorbed on the surface of PANI/ECs when the initial pH at 3.0, and the chromium exists in form of Cr(III).⁴³ No Cr(VI) was detected on the PANI/ECs by the XPS Cr 2p spectra. The result suggests that all Cr(VI) adsorbed on the surface of PANI/ECs has been reduced to Cr(III). However, almost no chromium was detected on the surface of PANI/ECs by Cr 2p XPS spectra with an initial pH of 1.0, indicating that the Cr(III) reduced from Cr(VI) can not be adsorbed on the surface of PANI/ECs. The peak of N 1s spectra of Cr(VI) adsorbed PANI/ECs (Figure 9B) has been deconvoluted to two major components at 397.6 and 399.0 eV, which are attributed to the imine group ($-\text{N}=\text{}$) and amine group ($-\text{NH}-$), respectively. The amine groups are oxidized to imine groups after being treated with Cr(VI) solution. Generally, the Cr(VI) adsorbed on the PANI/ECs has been reduced to Cr(III) by the amine groups, leading to the transformation of PANI from EB form to PB form. This result is consistent with the results based on FT-IR (Figure 8). The peak of C 1s spectra of Cr(VI) adsorbed PANI/ECs (Figure 9C) has been deconvoluted to three major components at 281.7, 283.2, and 285.1 eV, which are attributed to the C–N, C–O, and C–C or C=C, respectively.³¹ The intensity of peak at 283.0 eV assigned to C–O is increased after treated with Cr(VI), compared with that of PANI/ECs before treated with Cr(VI) (Figure 3B). This indicates that the EC has also involved in the reduction of Cr(VI) to Cr(III), which is consistent with the result based on the FT-IR (Figure 8).

The Cr(VI) and total Cr(VI) concentrations remained in the solutions after adsorption were also measured with an initial Cr(VI) concentrations of 1.0 mg/L (data were not showed)

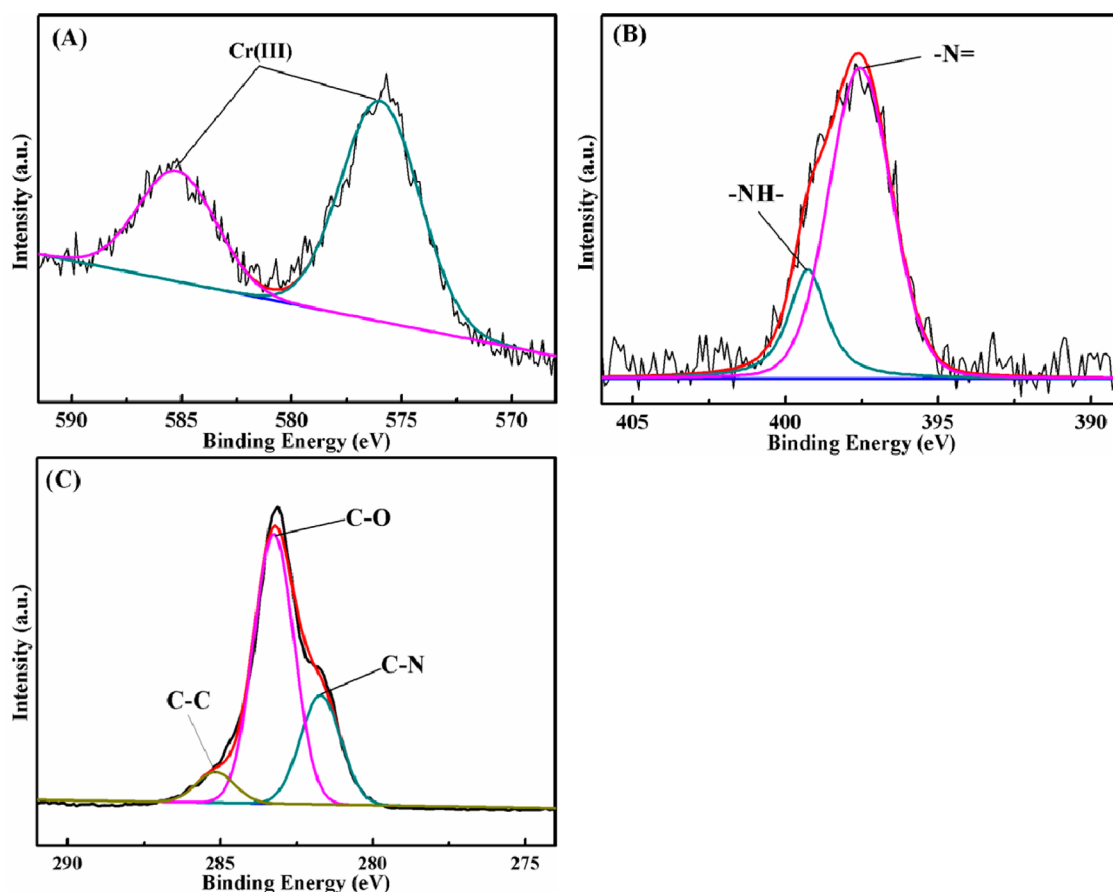


Figure 9. (A) Cr 2p, (B) N 1s, and (C) C 1s XPS spectra of the PANI/ECs with 20.0 wt % PANI loading after treated with 1000 mg/L Cr(VI) at pH 3.0 for 30 min.

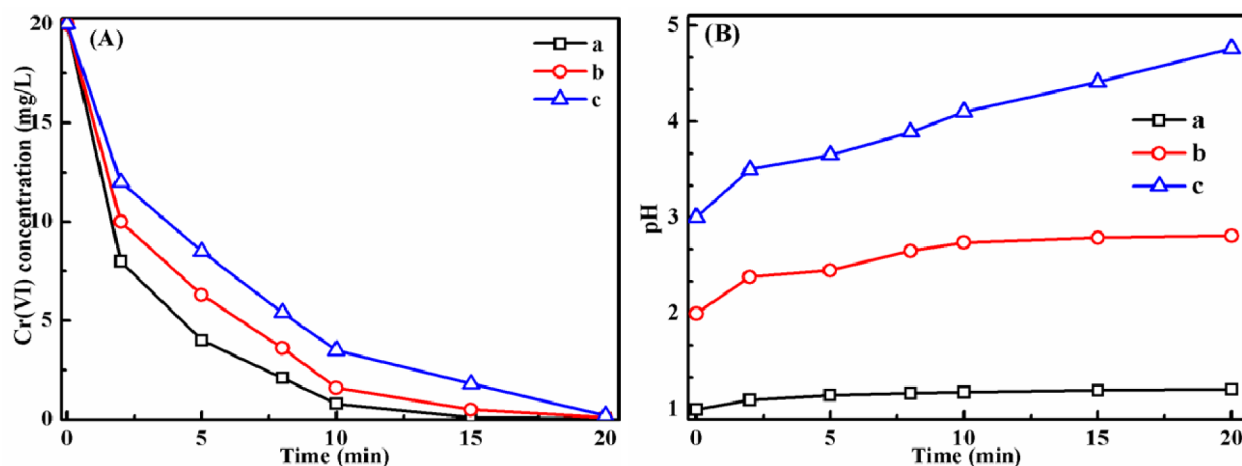
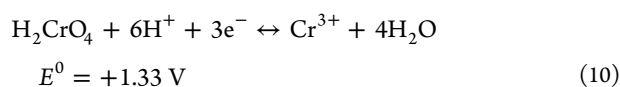
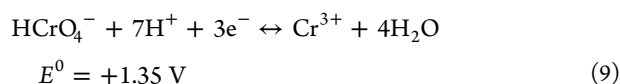
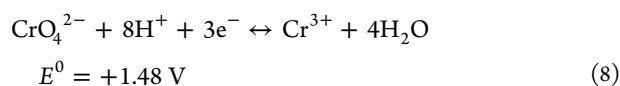
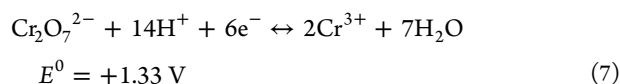


Figure 10. Reaction time dependent on (A) Cr(VI) concentration and (B) corresponding pH value in the bulk solutions with an initial pH value of (a) 1.0, (b) 2.0, and (c) 3.0.

with pH at 1.0, 2.0, and 3.0. No Cr(VI) was detected in all the solutions after treated by PANI/ECs, while 875 and 326 $\mu\text{g/L}$ of Cr(III) were detected in the solution with an initial pH of 1.0 and 2.0, respectively, suggesting that the Cr(VI) was totally reduced to Cr(III) and was released to the solution again. However, for the solution with an initial pH of 3.0, both Cr(VI) and Cr(III) were not detected in the solution after treated by PANI/ECs, indicating that all the Cr(III) were adsorbed on the surface of PANI/ECs. This is consistent with the result of the XPS (Figure 9). This is related to the pH value of solutions

after treated and the surface property of the adsorbent. As documented, the forms of Cr(III) are highly dependent on the pH value of the solution.⁹ Cr^{3+} is the dominant species when pH is below 4, monovalent $\text{Cr}(\text{OH})_2^+$ and divalent $\text{Cr}(\text{OH})_2^{2+}$ are dominant within the pH range 4–8.5, and then, $\text{Cr}(\text{OH})_3$ and $\text{Cr}(\text{OH})_4^-$ are dominant at pH higher than 8.5. The isoelectric point of PANI, the pH at which the particle surface carries no net electrical charge, is located around pH 4.0.⁴² The PANI was negatively charged through the deprotonation of the amine group (eq 3) when the pH was above 4.0, leading to

Cr(III) removal by the electrostatic attraction between the negatively charged PANI and the positively charged Cr(III). On the other hand, EC contains abundant $-OH$ groups (Figure 2), which can act as the active adsorption sites for the precipitation of positively charged Cr(III) ions. The isoelectric point of EC is around pH 2.5,⁴⁴ which is much lower than that of PANI. Furthermore, the EC, accounting for 80.0 wt % of the composites, might lead to an obvious decrease in the isoelectric point of PANI/ECs, which improves the electrostatic attraction of positively charged Cr(III) onto the surface of composites. The role of protons in Cr(VI) removal was also investigated in this study. As shown in Figure 10B, the protons were consumed for the reduction of Cr(VI). The final pH value was around 1.2 and 2.8 after complete reduction of Cr(VI) in the solution with an initial pH of 1.0 and 2.0. It was noticed that most of the protons were consumed during the initial 5 min, which was consistent with the finding that most Cr(VI) was removed in the initial 5 min (Figure 6A). This indicates that the protons were needed for the Cr(VI) reduction. Furthermore, three electrons are needed for the reduction of one Cr(VI) to Cr(III). This likely results from the complex participation of protons in eqs 7–10.⁴⁵



After treatment with PANI/ECs, the Cr(III) remaining in the solution is positively charged. However, the PANI/ECs are also positively charged at pH 1.2 and 2.8, leading to the release of Cr^{3+} to the solution by electrostatic repulsion. The pH value is 5.3 after being treated by PANI/ECs with an initial pH of 3.0, resulting in the adsorption of Cr^{3+} and $\text{Cr}(\text{OH})^{2+}$ by the electrostatic attraction. These were consistent with the fact that the Cr(III) reduced from the Cr(VI) at an initial pH value of 3.0 was completely adsorbed on the surface of PANI/ECs. This indicates that the Cr(VI) can be completely removed by PANI/ECs with one step when the initial pH is above 3.0.

On the basis of FT-IR and XPS analysis, the mechanisms involved in Cr(VI) removal by PANI/ECs are proposed. First, the functional groups (amine group) on the surface of the adsorbent are protonated to be positively charged, and then, they form surface complexes with the negatively charged Cr(VI) through electrostatic attraction. The Cr(VI) is reduced to Cr(III) by the oxidation of amine groups and hydroxyl groups of PANI/ECs. The protons are also consumed during the reduction process. The Cr(III) can be further adsorbed on the surface of PANI/ECs by electrostatic attraction. Moreover, the proton consumption has improved the Cr(III) adsorption.

CONCLUSION

The synthesized PANI/ECs have demonstrated a great performance on Cr(VI) removal with a 20.0 wt % PANI loading. Cr(VI) can be completely removed by 60 mg PANI/

ECs with a PANI loading of 20.0 wt % within 5 min from 20 mL of 2.0 mg/L solution, indicating that it can be used for fast Cr(VI) removal. The PANI/ECs exhibited a better Cr(VI) removal performance in acidic conditions. The better fitting with the pseudo-second-order model indicates the chemical adsorption of Cr(VI) by PANI/ECs. The PANI/ECs adsorbents follow Langmuir model better with calculated maximum adsorption capacities of 19.49, 26.11, and 38.76 mg/g for the 5.0, 10.0, and 20.0 wt % PANI/ECs. The introduction of PANI has improved the hydrophilicity of adsorbents, and enhanced the Cr(VI) reduction to Cr(III). Moreover, protons have been consumed and the pH value has increased obviously during the Cr(VI) reduction, which improved the Cr(III) adsorption on the surface of PANI/ECs. This indicates that the PANI/ECs can completely remove Cr(VI) from solution by two continuous steps of Cr(VI) reduction to Cr(III) and the Cr(III) adsorption on the surface of PANI/ECs.

ASSOCIATED CONTENT

Supporting Information

SEM image of PANI. This material is available free of charge via the Internet at <http://pubs.acs.org>.

AUTHOR INFORMATION

Corresponding Authors

*E-mail: suying.wei@lamar.edu (S.W.).

*E-mail: sundezhi@bjfu.edu.cn (D.S.).

*E-mail: xfwang@tongji.edu.cn (X.W.).

*E-mail: zhanhu.guo@lamar.edu or nanomaterials2000@gmail.com (Z.G.).

Notes

The authors declare no competing financial interest.

ACKNOWLEDGMENTS

This project is financially supported by the Texas Hazardous Waste Research Center (THWRC), the National Science Foundation-Chemical and Biological Separation under the EAGER program (CBET 11-37441) managed by Dr Rosemarie D. Wesson, the Materials Processing and Manufacturing program (CMMI 10-30755), and a Research Enhancement Grant (REG) of Lamar University. B.Q. acknowledges support from the China Scholarship Council (CSC) program.

REFERENCES

- (1) Gu, H.; Rapole, S. B.; Huang, Y.; Cao, D.; Luo, Z.; Wei, S.; Guo, Z. Synergistic Interactions between Multi-walled Carbon Nanotubes and Toxic Hexavalent Chromium. *J. Mater. Chem. A* **2013**, *1* (6), 2011–2021.
- (2) Zhu, J.; Wei, S.; Gu, H.; Rapole, S. B.; Wang, Q.; Luo, Z.; Haldolaarachchige, N.; Young, D. P.; Guo, Z. One-Pot Synthesis of Magnetic Graphene Nanocomposites Decorated with Core@Double-shell Nanoparticles for Fast Chromium Removal. *Environ. Sci. Technol.* **2011**, *46* (2), 977–985.
- (3) Xu, C.; Qiu, B.; Gu, H.; Yang, X.; Wei, H.; Huang, X.; Wang, Y.; Rutman, D.; Cao, D.; Bhana, S.; Guo, Z.; Wei, S. Synergistic Interactions between Activated Carbon Fabrics and Toxic Hexavalent Chromium. *ECS J. Solid State Sci. Technol.* **2014**, *3* (3), M1–M9.
- (4) Lin, C. J.; Wang, S. L.; Huang, P. M.; Tzou, Y. M.; Liu, J. C.; Chen, C. C.; Chen, J. H.; Lin, C. Chromate Reduction by Zero-valent Al Metal as Catalyzed by Polyoxometalate. *Water Res.* **2009**, *43* (20), 5015–5022.
- (5) Rengaraj, S.; Joo, C. K.; Kim, Y.; Yi, J. Kinetics of Removal of Chromium from Water and Electronic Process Wastewater by Ion

Exchange Resins: 1200H, 1500H and IRN97H. *J. Hazard. Mater.* **2003**, *102* (2–3), 257–275.

(6) Modrzejewska, Z.; Kaminski, W. Separation of Cr(VI) on Chitosan Membranes. *Ind. Eng. Chem. Res.* **1999**, *38* (12), 4946–4950.

(7) Qian, A.; Liao, P.; Yuan, S.; Luo, M. Efficient Reduction of Cr(VI) in Groundwater by a Hybrid Electro-Pd Process. *Water Res.* **2014**, *48*, 326–334.

(8) Hsu, L. C.; Wang, S. L.; Lin, Y. C.; Wang, M. K.; Chiang, P. N.; Liu, J. C.; Kuan, W. H.; Chen, C. C.; Tzou, Y. M. Cr(VI) Removal on Fungal Biomass of *Neurospora Crassa*: the Importance of Dissolved Organic Carbons Derived from the Biomass to Cr(VI) Reduction. *Environ. Sci. Technol.* **2010**, *44* (16), 6202–6208.

(9) Sun, X. F.; Ma, Y.; Liu, X. W.; Wang, S. G.; Gao, B. Y.; Li, X. M. Sorption and Detoxification of Chromium(VI) by Aerobic Granules Functionalized with Polyethylenimine. *Water Res.* **2010**, *44* (8), 2517–2524.

(10) Melitas, N.; Chuffe-Moscoco, O.; Farrell, J. Kinetics of Soluble Chromium Removal from Contaminated Water by Zerovalent Iron Media: Corrosion Inhibition and Passive Oxide Effects. *Environ. Sci. Technol.* **2001**, *35* (19), 3948–3953.

(11) Olad, A.; Nabavi, R. Application of Polyaniline for the Reduction of Toxic Cr(VI) in Water. *J. Hazard. Mater.* **2007**, *147* (3), 845–851.

(12) Mitra, P.; Sarkar, D.; Chakrabarti, S.; Dutta, B. K. Reduction of Hexa-valent Chromium with Zero-valent Iron: Batch Kinetic Studies and Rate Model. *Chem. Eng. J.* **2011**, *171* (1), 54–60.

(13) Gu, H.; Rapole, S. B.; Sharma, J.; Huang, Y.; Cao, D.; Colorado, H. A.; Luo, Z.; Haldolaarachchige, N.; Young, D. P.; Walters, B.; Wei, S.; Guo, Z. Magnetic Polyaniline Nanocomposites toward Toxic Hexavalent Chromium Removal. *RSC Adv.* **2012**, *2* (29), 11007–11018.

(14) Zhu, J.; Gu, H.; Guo, J.; Chen, M.; Wei, H.; Luo, Z.; Colorado, H. A.; Yerra, N.; Ding, D.; Ho, T. C.; Haldolaarachchige, N.; Hopper, J.; Young, D. P.; Guo, Z.; Wei, S. Mesoporous Magnetic Carbon Nanocomposite Fabrics for Highly Efficient Cr(VI) Removal. *J. Mater. Chem. A* **2014**, *2* (7), 2256–2265.

(15) Lin, Y. C.; Wang, S. L. Chromium(VI) Reactions of Polysaccharide Biopolymers. *Chem. Eng. J.* **2012**, *181–182*, 479–485.

(16) Wang, S. L.; Lee, J. F. Reaction Mechanism of Hexavalent Chromium with Cellulose. *Chem. Eng. J.* **2011**, *174* (1), 289–295.

(17) Tang, L.; Yang, G.-D.; Zeng, G.-M.; Cai, Y.; Li, S.-S.; Zhou, Y.-Y.; Pang, Y.; Liu, Y.-Y.; Zhang, Y.; Luna, B. Synergistic Effect of Iron Doped Ordered Mesoporous Carbon on Adsorption-coupled Reduction of Hexavalent Chromium and the Relative Mechanism Study. *Chem. Eng. J.* **2014**, *239*, 114–122.

(18) Gupta, V. K.; Agarwal, S.; Saleh, T. A. Chromium Removal by Combining the Magnetic Properties of Iron Oxide with Adsorption Properties of Carbon Nanotubes. *Water Res.* **2011**, *45* (6), 2207–2212.

(19) Fu, F.; Ma, J.; Xie, L.; Tang, B.; Han, W.; Lin, S. Chromium Removal using Resin Supported Nanoscale Zero-valent Iron. *J. Environ. Manag.* **2013**, *128*, 822–827.

(20) Liu, T.; Zhao, L.; Sun, D.; Tan, X. Entrapment of Nanoscale Zero-valent Iron in Chitosan Beads for Hexavalent Chromium Removal from Wastewater. *J. Hazard. Mater.* **2010**, *184* (1–3), 724–730.

(21) Geng, B.; Jin, Z.; Li, T.; Qi, X. Kinetics of Hexavalent Chromium Removal from Water by Chitosan-Fe⁰ Nanoparticles. *Chemosphere.* **2009**, *75* (6), 825–830.

(22) Liu, X.; Qian, X.; Shen, J.; Zhou, W.; An, X. An Integrated Approach for Cr(VI)-detoxification with Polyaniline/Cellulose Fiber Composite Prepared using Hydrogen Peroxide as Oxidant. *Bioresour. Technol.* **2012**, *124*, 516–519.

(23) Zhou, Y.; Jin, Q.; Zhu, T.; Akama, Y. Adsorption of Chromium (VI) from Aqueous Solutions by Cellulose Modified with β -CD and Quaternary Ammonium Groups. *J. Hazard. Mater.* **2011**, *187* (1–3), 303–310.

(24) Chiou, N. R.; Epstein, A. J. Polyaniline Nanofibers Prepared by Dilute Polymerization. *Adv. Mater.* **2005**, *17* (13), 1679–1683.

(25) Kumar, P. A.; Chakraborty, S. Fixed-bed Column Study for Hexavalent Chromium Removal and Recovery by Short-chain Polyaniline Synthesized on Jute Fiber. *J. Hazard. Mater.* **2009**, *162* (2–3), 1086–1098.

(26) Ruotolo, L. A. M.; Gubulin, J. C. Chromium(VI) Reduction using Conducting Polymer Films. *React. Funct. Polym.* **2005**, *62* (2), 141–151.

(27) Liu, X.; Zhou, W.; Qian, X.; Shen, J.; An, X. Polyaniline/Cellulose Fiber Composite Prepared Using Persulfate as Oxidant for Cr(VI)-detoxification. *Carbohydr. Polym.* **2013**, *92* (1), 659–661.

(28) Li, G.; Martinez, C.; Semancik, S. Controlled Electrophoretic Patterning of Polyaniline from a Colloidal Suspension. *J. Am. Chem. Soc.* **2005**, *127* (13), 4903–4909.

(29) Stejskal, J.; Sapurina, I.; Trchová, M.; Konyushenko, E. N. Oxidation of Aniline: Polyaniline Granules, Nanotubes, and Oligoaniline Microspheres. *Macromolecules.* **2008**, *41* (10), 3530–3536.

(30) Mavinakuli, P.; Wei, S.; Wang, Q.; Karki, A. B.; Dhage, S.; Wang, Z.; Young, D. P.; Guo, Z. Polypyrrole/Silicon Carbide Nanocomposites with Tunable Electrical Conductivity. *J. Phys. Chem. C* **2010**, *114* (9), 3874–3882.

(31) Beard, B. C.; Spellane, P. XPS Evidence of Redox Chemistry between Cold Rolled Steel and Polyaniline. *Chem. Mater.* **1997**, *9* (9), 1949–1953.

(32) Kang, E. T.; Neoh, K. G.; Tan, K. L. Polyaniline: A Polymer with Many Interesting Intrinsic Redox States. *Prog. Polym. Sci.* **1998**, *23* (2), 277–324.

(33) Zhu, J.; Wei, S.; Zhang, L.; Mao, Y.; Ryu, J.; Haldolaarachchige, N.; Young, D. P.; Guo, Z. Electrical and Dielectric Properties of Polyaniline-Al₂O₃ Nanocomposites Derived from Various Al₂O₃ Nanostructures. *J. Mater. Chem.* **2011**, *21* (11), 3952–3959.

(34) Javadi, A.; Zheng, Q.; Payen, F.; Javadi, A.; Altin, Y.; Cai, Z.; Sabo, R.; Gong, S. Polyvinyl Alcohol-Cellulose Nanofibrils-Graphene Oxide Hybrid Organic Aerogels. *ACS Appl. Mater. Inter.* **2013**, *5* (13), 5969–5975.

(35) Aggour, Y. A. Thermal Decomposition Behaviour of Ethyl Cellulose Grafted Copolymers in Homogeneous Media. *J. Mater. Sci.* **2000**, *35* (7), 1623–1627.

(36) Taha, A. A.; Wu, Y.; Wang, H.; Li, F. Preparation and Application of Functionalized Cellulose Acetate/Silica Composite Nanofibrous Membrane via Electrospinning for Cr(VI) Ion Removal from Aqueous Solution. *J. Environ. Manag.* **2012**, *112*, 10–16.

(37) Kalidhasan, S.; Santhana KrishnaKumar, A.; Rajesh, V.; Rajesh, N. Ultrasound-assisted Preparation and Characterization of Crystalline Cellulose-ionic Liquid Blend Polymeric Material: A Prelude to the Study of its Application toward the Effective Adsorption of Chromium. *J. Colloid Interface Sci.* **2012**, *367* (1), 398–408.

(38) Kalidhasan, S.; Gupta, P. A.; Cholleti, V. R.; Santhana Krishna Kumar, A.; Rajesh, V.; Rajesh, N. Microwave Assisted Solvent Free Green Preparation and Physicochemical Characterization of Surfactant-anchored Cellulose and its Relevance toward the Effective Adsorption of Chromium. *J. Colloid Interface Sci.* **2012**, *372* (1), 88–98.

(39) Li, Y.; Zhu, S.; Liu, Q.; Chen, Z.; Gu, J.; Zhu, C.; Lu, T.; Zhang, D.; Ma, J. N-doped Porous Carbon with Magnetic Particles Formed In Situ for Enhanced Cr(VI) Removal. *Water Res.* **2013**, *47* (12), 4188–4197.

(40) Lee, G.; Park, J.; Harvey, O. R. Reduction of Chromium(VI) mediated by Zero-valent Magnesium under Neutral pH Conditions. *Water Res.* **2013**, *47* (3), 1136–1146.

(41) Liu, T.; Yang, X.; Wang, Z.-L.; Yan, X. Enhanced Chitosan Beads-supported FeO-Nanoparticles for Removal of Heavy Metals from Electroplating Wastewater in Permeable Reactive Barriers. *Water Res.* **2013**, *47* (17), 6691–6700.

(42) Wang, J.; Zhang, K.; Zhao, L. Sono-assisted Synthesis of Nanostructured Polyaniline for Adsorption of Aqueous Cr(VI): Effect of Protonic Acids. *Chem. Eng. J.* **2014**, *239*, 123–131.

(43) Park, D.; Yun, Y. S.; Park, J. M. XAS and XPS Studies on Chromium-binding Groups of Biomaterial During Cr(VI) Biosorption. *J. Colloid Interface Sci.* **2008**, *317* (1), 54–61.

- (44) Wang, J.; Somasundaran, P. Mechanisms of Ethyl(hydroxyethyl) Cellulose–solid Interaction: Influence of Hydrophobic Modification. *J. Colloid Interface Sci.* **2006**, *293* (2), 322–332.
- (45) Park, D.; Yun, Y. S.; Park, J. M. Reduction of Hexavalent Chromium with the Brown Seaweed *Ecklonia* Biomass. *Environ. Sci. Technol.* **2004**, *38* (18), 4860–4864.